STScI | SPACE TELESCOPE SCIENCE INSTITUTE

Instrument Science Report COS 2022-08(v1)

Cycle 28 COS/FUV Spectroscopic Sensitivity Monitor

Kate Rowlands 1[1], Ravi Sankrit[2]

[1] Space Telescope Science Institute, Baltimore, MD

8 August 2022

ABSTRACT

The Cycle 28 COS/FUV spectroscopic sensitivity monitor ran from December 2020 to October 2021. Observations of the standard modes and the new modes (G160M/1533 and G140L/800, introduced in Cycle 26) were obtained at Lifetime Position 4 (LP4), the nominal position for COS starting October 2, 2017, and the blue modes (G130M/1055 and G130M/1096) were obtained at Lifetime Position 2 (LP2). Connection visits to LP5 and LP3 were obtained in preparation for the start of G130M/1291 (and longwards) at LP5, and G140L/800 at LP3. The Time-Dependent Sensitivity (TDS) slopes of all modes ranged from 0% *to* -3% *per year. In this ISR we describe the program and its execution, and provide a summary of the analysis and results. Based on the change in the net count rates over a one year timescale, we find that the FUV TDS does not depend on LP between LP4 and LP5.*

Contents

1. Introduction

The throughput of the COS FUV detector changes with time (Osten et al. 2010), and this is monitored with the COS FUV spectroscopic sensitivity calibration program. Previous programs and their results are detailed in Osten et al. (2011), Bostroem et al. (2015), De Rosa et al. (2016, 2017, 2018), Sankrit (2019, 2020), Sankrit & Rowlands (2021). Sensitivity variations over time are modeled as a function of wavelength for each cenwave and segment (FUVA, FUVB). These are included in the TDS reference file (TDSTAB) for use in CalCOS to obtain flux calibrated data, when paired with the photometric throughput reference file (FLUXTAB).

The Cycle 28 FUV TDS monitor (PID: 16324, PI: K. Rowlands) consisted of observations of the flux calibration standards, GD71 and WD0308-565, with the plan of obtaining data every two months between December 2020 and October 2021. We also checked the consistency of the time-dependent sensitivity between LP5 and the previous lifetime position LP4 for G130M/1291 (and longwards), and for LP3 and the previous lifetime position LP4 for G140L/800.

2. Program design

The Time-Dependent Sensitivity (TDS) monitoring program observes the bluest and reddest central wavelengths of each grating, with additional coverage of the G130M/1055 and 1096 blue modes, G130M/1222, and the new cenwaves G160M/1533 and G140L/800 that were added in Cycle 26. The white dwarf standard stars WD0308-565 and GD71 have been used for monitoring since Cycle 20, and are currently observed every two months. The modes tracked in Cycle 28 are listed in Tables 1 and 2. The targets for each cenwave and segment are chosen to optimize the signal-to-noise ratio and to minimize the impact on detector lifetime. When GD71 is not observable from mid-April to early August, exposures are obtained solely with WD0308-565.

Exposure times were determined by requiring a S/N of 15 per resel at the wavelength of least sensitivity for all modes, except the blue modes, G130M/1222, and G140L/800. For the blue modes and for G130M/1222, the goal was to obtain S/N$= 25$ per resel at the wavelength of maximum sensitivity, ensuring S/N> 15 for > 1030Å for G130M/1096/FUVB, and for > 1130Å for G130M/1055/FUVA and G130M/1222. For G140L/800, the target S/N was 15 per resel at the wavelength of least sensitivity longwards of 1150Å, below which there is a sharp drop in throughput. At < 1150Å the exposure time obtains a S/N of 30–40 per 20Å bin.

Table 1. Modes Tracked using GD71.

Grating	Cenwave	Segment	t_{exp} (sec)
G130M	1096	FUVB[a]	744
G160M	1533	FUVA	106
	1577	FUVA	135
	1623	FUVA	177

[a]G130M/1096 is observed with segment FUVB only since the target is too bright to be observed with segment FUVA.

The exposure times and overheads require two orbits per visit for GD71 and three orbits per visit for WD0308-565. There are no wavelength calibration lamp lines available in the wavelength range covered by G130M/1096/FUVB, so the visits include a GO wavelength calibration lamp observation taken at the same Optics Select Mechanism 1 (OSM1) position immediately after the science exposure using segment FUVA.

The standard mode and new cenwave observations were obtained at the nominal (current) COS FUV lifetime position (LP4), while the blue modes were observed at LP2. COS FUV G130M operations for cenwave 1291 and longwards transitioned from LP4 to LP5 at the beginning of Cycle 29, on 2021 October 4. Two closely spaced observations of WD0308-565 at LP4 and LP5, and LP4 and LP3 were included as part of the Cycle 28 program. These connection exposures, taken within the same visit, establish the scaling between the net counts for LP4 and LP5, and LP4 and LP3, and were scheduled 4 and 14 weeks apart from the LP5 and LP3 visits of the fluxes and flats program (PID 16466, Sankrit et al. 2022). All observations were obtained at FP-POS $= 3$. The visit structure was unchanged from Cycle 27, except for the addition of the LP3 and LP5 connection exposures in visits 05 and 07 (see Table 3).

3. Observations

The data used in the FUV TDS analysis use the observations shown in Table 3, sorted by observation date. The program included six visits for WD0308-565, and five for GD71, which is not visible between the end of April and the beginning of August. The program was impacted by one failed visit, 03, on 2021 Februrary 23, and the observations were repeated three weeks later on 2022 March 15 in visit 53. Note that the execution of visit 10 was rescheduled from October to December due to an anomaly with *HST*. The failed and rescheduled visits had no impact on the TDS monitoring. All of the data from successful observations are available in the archive.

Table 2. Modes Tracked using WD0308-565.

Grating	Cenwave	Segment	t_{exp} (sec)
G130M	1055	Both	393
	1222	Both	267
	1291	Both	236
	1327[a]	FUVA	274
G160M	1533	FUVB	223
	1577	FUVB	275
	1623	FUVB	372
G140L	800[a]	FUVA	367
	1105[a]	FUVA	332
	1280	Both	366

[a]Cenwaves 1327, 800, and 1105 are FUVA-only.

Table 3. Observation dates for PID 16324.

Obs. Date	Visit No.	Target
2020-12-26	02	GD71
2020-12-27	01	WD0308-565
2021-02-18	04	WD0308-565
2021-03-15	53	WD0308-565
2021-04-10	06	GD71
2021-04-21†	05	WD0308-565
2021-06-08⋆	07	WD0308-565
2021-08-11	08	WD0308-565
2021-08-15	09	GD71
2021-10-16	11	GD71
2021-12-07	10	WD0308-565

†LP4–LP5 connection visit.

⋆LP4–LP3 connection visit.

4. Analysis and Results

4.1 Regular TDS monitor

The data were analyzed using the TDS analysis code as described in Bostroem et al. (2015), using calibrated `x1d.fits` files from previous monitoring programs from September 2009–December 2021. Net counts were binned over 20Å for the low resolution modes, and over 5Å for the medium resolution modes. With this S/N, we aimed to achieve a flux calibration accuracy of 5% absolute and 2% relative. The data obtained at LP2, LP3, LP4 and LP5 are scaled to data obtained at LP1, LP2, LP3 and LP4, respectively using the connection observations obtained at the different LPs. Fits to the data using a piecewise-linear function were preformed with breakpoints at decimal years 2010.20, 2011.20, 2011.75, 2012.00, 2012.80, 2013.80, 2015.5 and 2019.0. The overall relative sensitivity was normalized to 1.0 at the time of first light (May 01, 2009). Fig 1 shows a summary plot of the sensitivity against time, along with the solar activity towards Earth as a function of time. The 10.7 cm solar fluxes are obtained from the Solar Monitoring Program hosted by Natural Resources Canada at ftp://ftp.seismo.nrcan.gc.ca/spaceweather/solar_flux/daily_flux_values/. Monitoring of the solar flux is important since previous steepenings of the FUV TDS slopes have been correlated with high solar activity (Bostroem et al. 2015). The TDS slopes since 2019.0 have been stable and typically varied between 0 and -3% per year, and are relatively uniform with wavelength, as shown in Figure 2.

4.2 LP4–LP5 scaling

The TDS is assumed to be independent of LP, allowing the same TDS model to be applied at all LPs. Similar to Sankrit et al. (2019), we compare the fractional change in the count rates between two epochs for each cenwave observed at LP4 and LP5. The first epoch observations were obtained as part of the Cycle 28 FUV TDS program, while the second epoch observations were obtained as part of the Cycle 29 FUV TDS program (PID 16830). The dates of the observations and the time intervals between the epochs are listed in Table 4, and the exposures used are listed in Table 5. Analysis of the dependence of the TDS between LP4 and LP3 for cenwave G140L/800 will be presented in Rowlands et al. in prep.

The fractional change in the net count rates from the calibrated `x1d.fits` files in % yr^{-1} is calculated as

$$\Delta C(t_1, t_2) = 100. \times ((C_{t_2} - C_{t_1})/C_{t_1}) \times 1/(t_2 - t_1), \quad (1)$$

where C_{t_1} and C_{t_2} are the count rates measured in the Epoch 1 and Epoch 2 data, respectively, and $t_2 - t_1$ is the time interval between the observations in years for each mode (Δt column in Table 4).

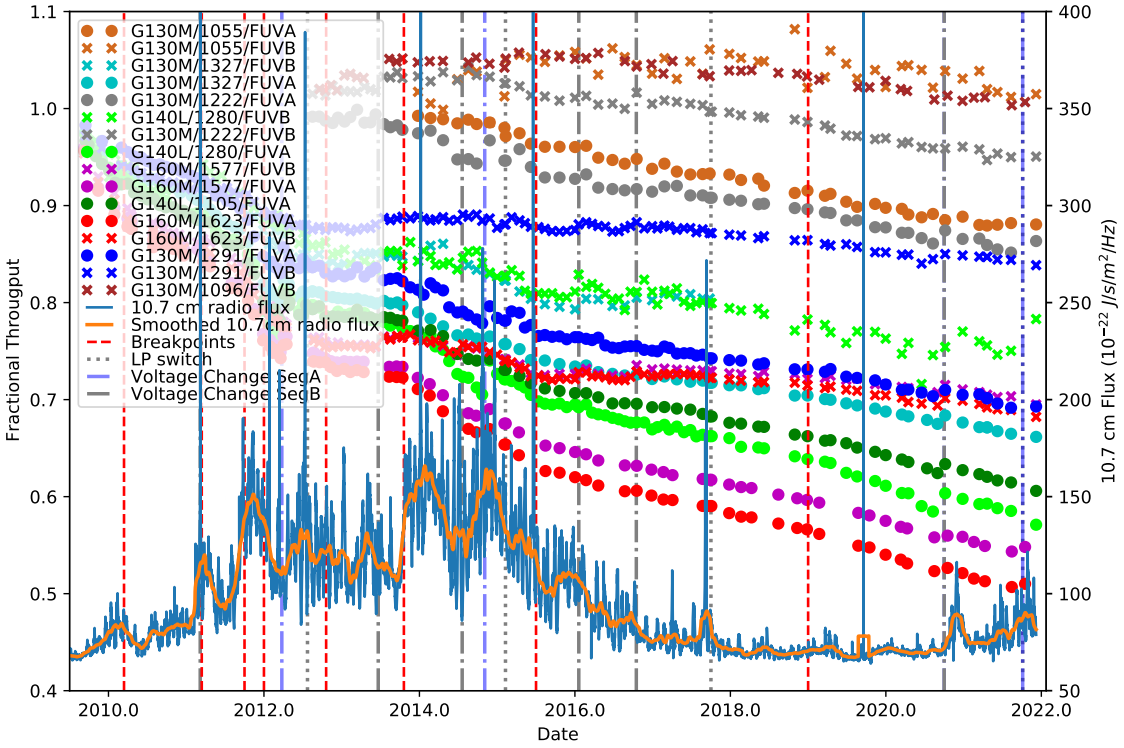

Figure 1. Changing sensitivity as a function of time for monitored COS FUV cenwaves (see legend). The solar flux incident at the Earth is overplotted, and is measured using the 10.7 cm radio flux (blue line: unsmoothed, orange line: smoothed). Dashed red vertical lines are breakpoints in the piece-wise linear function used to model the TDS, dotted grey vertical lines mark the LP moves, and dot-dashed vertical lines correspond to changes in operational voltage.

We plot the percentage change in net counts for LP4 and LP5 as a function of wavelength, and the difference in these changes, in Figure 3 for G130M/1291/FUVB, Figure 4 for G130M/1291/FUVA, and Figure 5 for G130M/1327/FUVA. If the TDS is independent of LP then the fractional change in net counts should be similar between LP4 and LP5. The count rates are similar and are typically within 2% of each other, except around detector edges and regions contaminated with airglow lines, where larger differences are seen between the LP4 and LP5 count rates. For G130M/1291/FUVB the count rate differences are typically centered on zero, although for segment FUVA for cenwaves G130M/1291 and 1327 the mean difference in the count rates shows a slight offset of -1.3% and -1.5% per year, respectively. This is because the operating voltage was raised on segment FUVA from 169 to 173 for LP4 on 2021 October 4, which resulted in a change in the net counts. This slight offset in net counts is consistent with what is observed from previous operating voltage increases. The differences in the count rates are consistent with our tolerance, therefore the TDS does not depend on LP based on LP4 and LP5 data.

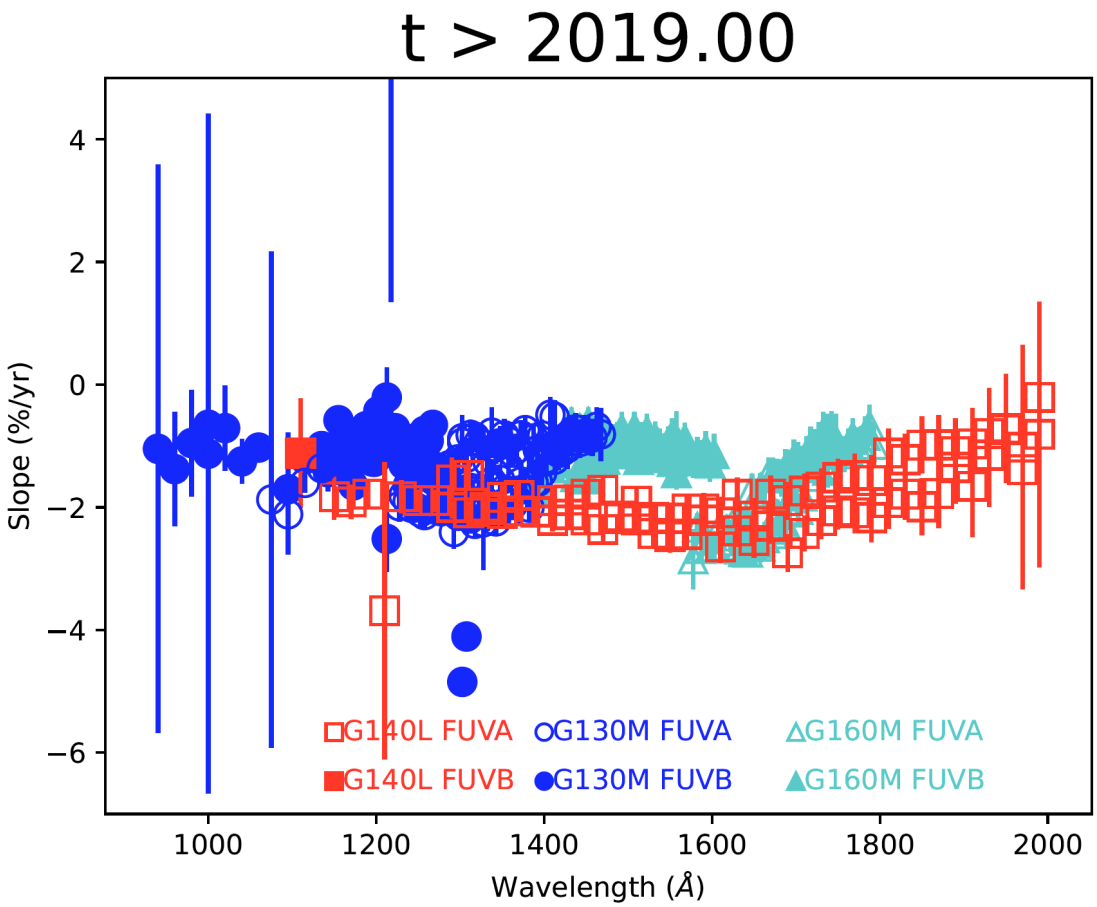

Figure 2. The FUV TDS slopes (percentage change per year) measured during Cycle 28 as a function of wavelength, for each grating and segment (see legend). The FUV TDS slopes were stable during the cycle, and typically varied between 0 and -3% per year. Uncertainties on the slopes are small at most wavelengths, but are larger near the detector edges and around airglow lines. Although G140L coverage extends down to 800Å, data is only included in the TDS slope plot longwards of 1100Å due to the low throughput of G140L/1280 FUVB at $<$ 1100Å, and G140L/800 is not included in the plot. Future updates to the TDS monitor may include the addition of G140L/800 data to extend to shorter wavelengths.

5. Continuation Plan

In Cycle 29, the regular monitoring of the FUV TDS continued in program 16830 (PI: K. Rowlands). The targets and frequency of visits are the same as in Cycle 28. Additional observations are planned to support the flux calibration of G160M that will start at LP6 in Cycle 30, along with the second pairs of LP4–LP3 and LP4–LP5 connection exposures. Additionally, we will monitor cenwave G160M/1611 to help disentangle the dependence of the TDS on detector position from its dependence on

Table 4. Dates and time intervals for the LP4/LP5 comparison.

Target	Lifetime Pos.	Cenwave	Epoch 1	Epoch 2	Δt (yr)
WD 0308-565	LP4	1291	2021-04-21	2022-06-06	1.126
WD 0308-565	LP5	1291	2021-04-21	2022-06-06	1.126
WD 0308-565	LP4	1327	2021-04-21	2022-04-16	0.986
WD 0308-565	LP5	1327	2021-04-21	2022-04-16	0.986

Table 5. Exposure ROOTNAMEs used for the LP4/LP5 comparison for G130M cenwaves.

Cenwave	Segment	LP4 (epoch 1)	LP4 (epoch 2)	LP5 (epoch 1)	LP5 (epoch 2)
1291	Both	lefe05o0q	ler107a7q	lefe05o2q	ler107a9q
1327	FUVA	lefe05piq	ler15bhaq	lefe05pkq	ler15bhcq

wavelength. The TDS slope shown by cenwave 1611 will be used to find the optimal weights between detector position and wavelength when averaging the TDS slopes of the regularly tracked cenwaves 1577 and 1623.

Acknowledgements

We thank Elaine Mae Frazer for help with the LP4–LP5 comparison.

Change History for COS ISR 2022-08

Version 1: 8 August 2022- Original Document

References

Bostroem, K. A., et al. 2015, COS Technical Instrument Reports 2014-05
De Rosa, G., Sana, H., Ely, J. and the COS team, 2016, COS Instrument Science Report 2016-13
De Rosa, G. and the COS team, 2017, COS Instrument Science Report 2017-10
De Rosa, G. and the COS team, 2018, COS Instrument Science Report 2018-09
Oliveira, C., et al. 2018, COS Instrument Science Report 2018-16
Osten, R. A., et al. 2010, COS Instrument Science Report 2010-15
Osten, R. A., et al. 2011, COS Instrument Science Report 2011-02

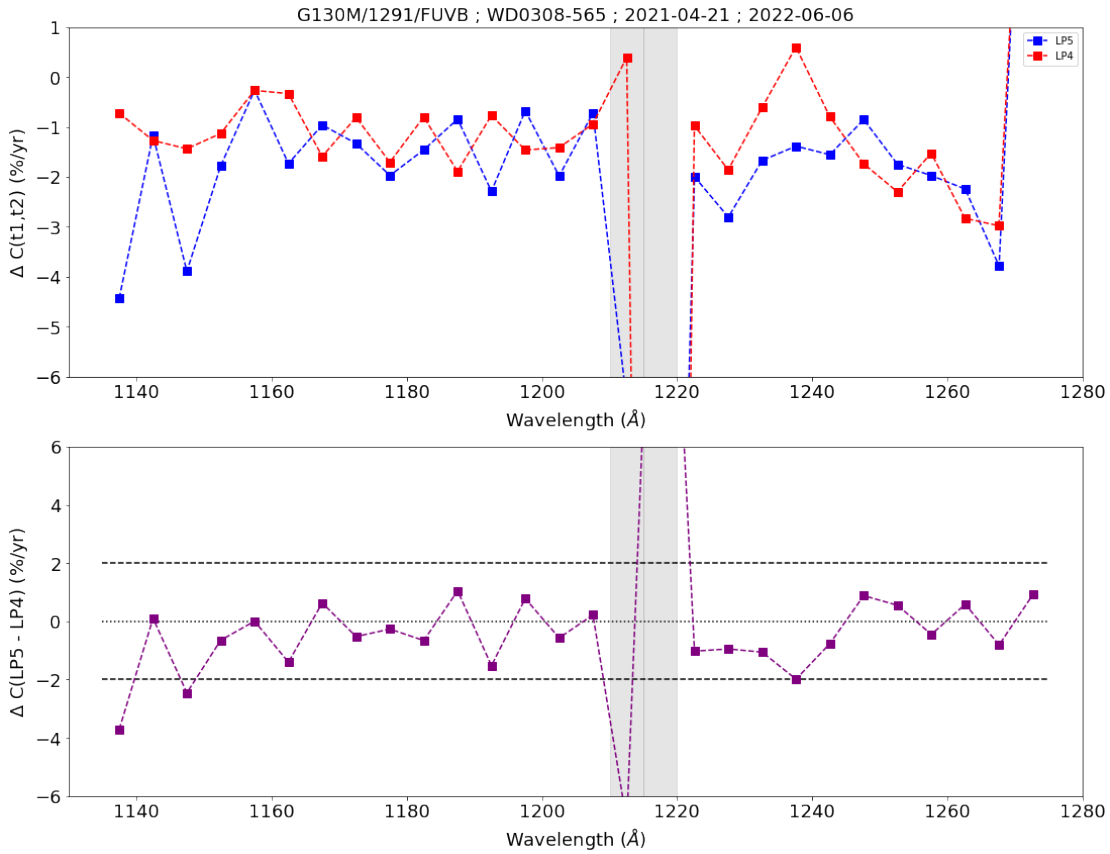

Figure 3. Results for G130M/1291, segment FUVB. Top panel: Changes in the net count rates at LP5 (blue squares) and LP4 (red squares), in % yr^{-1}, in 5Å bins. The grey shaded regions show wavelength ranges contaminated with airglow lines. The bottom panel shows the difference between the LP5 and LP4 net count rates also in % yr^{-1}.

Sankrit, R. 2019, COS Instrument Science Report 2019-18
Sankrit, R. 2020, COS Instrument Science Report 2020-06
Sankrit, R. & Rowlands, K., 2021, COS Instrument Science Report 2021-02

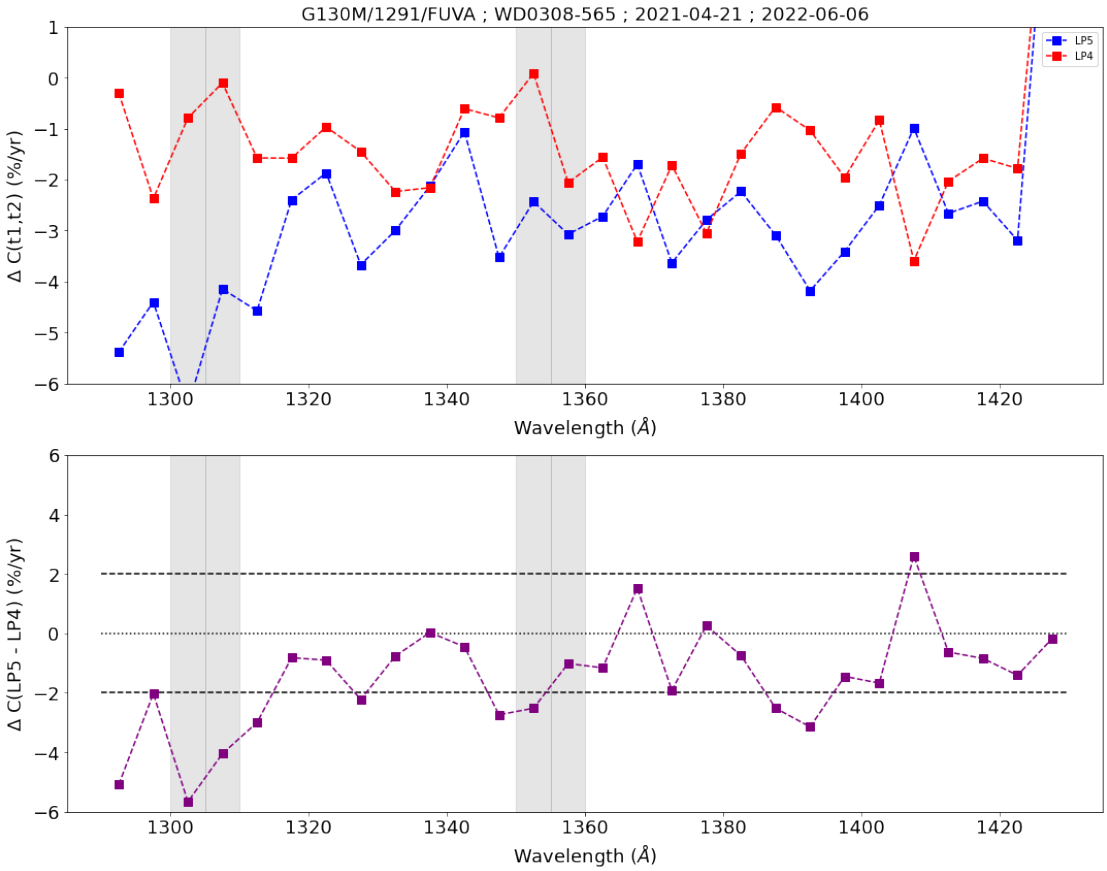

Figure 4. Results for G130M/1291, segment FUVA. Top panel: Changes in the net count rates at LP5 (blue squares) and LP4 (red squares), in % yr^{-1}, in 5Å bins. The grey shaded regions show wavelength ranges contaminated with airglow lines. The bottom panel shows the difference between the LP5 and LP4 net count rates also in % yr^{-1}.

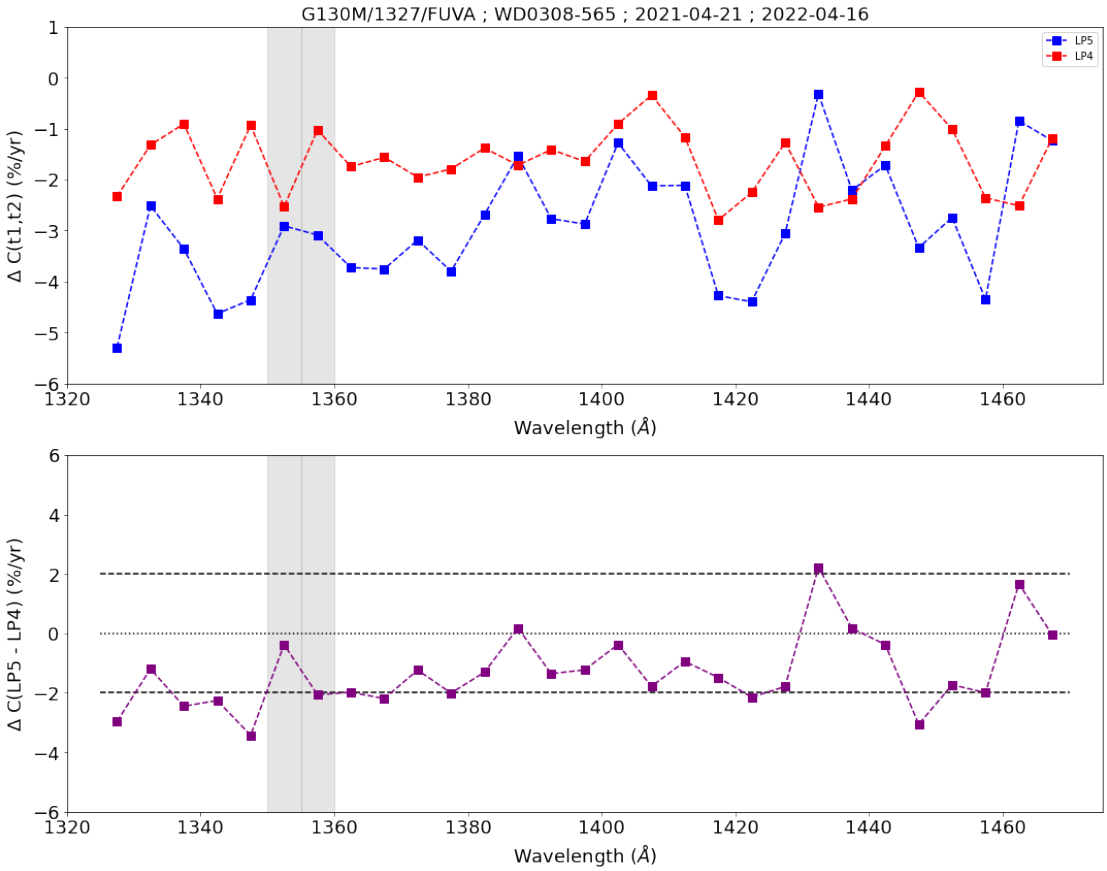

Figure 5. Results for G130M/1327, segment FUVA. Top panel: Changes in the net count rates at LP5 (blue squares) and LP4 (red squares), in % yr^{-1}, in 5Å bins. The grey shaded regions show wavelength ranges contaminated with airglow lines. The bottom panel shows the difference between the LP5 and LP4 net count rates also in % yr^{-1}.